Research paper

Experimental study on head-on collisions of detonation waves in insensitive high explosive

Xiangli Guo*, Yong Han*, Yushi Wen*, Kaiyuan Tan*, and Wei Cao*,**†

*Institute of Chemical Materials, China Academy of Engineering Physics, Mianyang, Sichuan 621999, CHINA
Phone: +86-816-2485366
†Corresponding author: weicao@caep.cn

**Department of Mechanical Engineering, McGill University, Montreal, Quebec H3A 0C3, CANADA

Received: April 10, 2018 Accepted: October 26, 2018

Abstract

In this paper, we experimentally studied the head-on collisions of detonation waves in a TATB (1,3,5-triamino-2,4,6-trinitrobenzene) based insensitive high explosive (IHE). A cuboid explosive charge was initiated from two opposite ends simultaneously, the breakout waveform of the detonation waves along the collision line and the line normal to the collision line was recorded by a high-speed streak camera. Results show that the corner-turning performance of TATB based explosives affects the waveform. Then, we measured the interface particle velocity histories of collision point by using LiF transparent window and photonic Doppler velocimetry (PDV). A longer run distance of detonation wave results in a higher particle velocity. Additionally, the incident detonation pressure was calculated on the basis of impedance matching equation. Compared with the explosive's Chapman-Jouguet (CJ) detonation pressure, it is inferred that the detonation waves are not fully built up in our experimental conditions.

Keywords: head-on collision, detonation waves, high insensitive explosive, detonation pressure

1. Introduction

Dynamic failure of ductile metals subjected to shock loading is of considerable interest for basic studies and engineering application in shock physics, where the energy source may originate from explosives detonation. Especially when an explosive charge is initiated from two opposite sides, the detonation waves counter propagates and collides. The head-on collisions of detonation waves (or shock waves) form regular reflection or irregular (i.e. Mach) reflection depending on the collision angles, and generate regions of high pressure and temperature which are localized in the immediate vicinity of the collision points. The resulting pressure can be more than the sum of the individual waves[1], and impose an intense impulsive load on the attached body or structure.

The basic theory of multi-wave intersections has been elaborated in monographs[2,3]. The experimental and numerical study on the head-on collisions of shock waves (or detonation waves) in gaseous media has been widely investigated in the past decades[4-7], while the head-on collisions of detonation waves in condensed explosives were less studied. Oppenheim et al.[8] gave a theoretical analysis on the dynamics of shock intersections in detonable gaseous media as well as in condensed (exactly, liquid) explosives, and the theoretical results were in satisfactory agreement with experimental records. Recently, many researchers used the detonation of high explosive to give an outward impulse to the attached thin metallic wall or plate, which expands with a high strain rate until rupture occurs[9-15]. Specially, when the high explosive is detonated from two opposite sides, a collision region with a higher pressure appears and sometimes a typical jet-like spiking is formed in this region as the attached metal ruptures[16,17]. However, few experiments report the waveform, interface particle velocity histories and pressure of the head-on collision region.

In this work, a cuboid TATB (1,3,5-triamino-2,4,6-trinitrobenzene) based insensitive high explosive (IHE) was initiated from two opposite ends, then the detonation waves counter propagated and collided. The detonation waveform and interface velocity histories on the head-on collision line were recorded by a high-speed streak camera

and photonic Doppler velocimetry (PDV)[18], respectively. Then the peak detonation pressure on that line was calculated using the impedance match equation. In addition, the dead zone for the unreactive explosive was identified.

2. Experimental

The cuboid main charges were machined from the isostatically pressed TATB based polymer bonded explosives (PBX-I, 95 wt% TATB and 5 wt% binder) with density of 1.895 ± 0.002 g·cm^{-3}. The dimension used in the waveform experiments was $100 \times 100 \times 60$ mm, and the dimensions used in the interface velocity measurements were $100 \times 100 \times 40$ mm and $100 \times 100 \times 20$ mm. The main charge was detonated at two opposite rectangle surfaces by two cylindrical pressed boosters (95 wt% HMX and 5 wt% binder, 1.860 ± 0.002 g·cm^{-3}, $\phi 20 \times 20$ mm) which were initiated by two detonators simultaneously. The experimental setup is illustrated in Figure 1.

In the waveform experiments, a high-speed rotating mirror streak camera (with writing speed of 3 mm·μs^{-1}, i.e., 60000 rpm) was used to catch the lighted images of the detonation wave from the collision line and the line normal to the collision line on the upper surface of the main charge, which are drawn in Figure 1 as AA' and BB' (dashed lines) dividing the surface equally. For each shot, just one lighted image from AA' or BB' was recorded. The LiF window was not mounted in this experiment, and the 2-mm-wide transparent adhesive tapes painted with the $Ba(NO_3)_2$ luminescence agent (granularity 0.12~0.18 mm) were glued along the lines to enhance the luminescence.

In the interface velocity experiments, the interface velocity histories between the detonating explosives and LiF transparent windows were measured by a PDV system, which can track velocity on nanosecond time scales. The Teledyne LeCroy digitizer (WaveMaster 816 Zi-B) was used in PDV measurements (40 GS/s, 16 GHz bandwidth). The velocity profiles were computed by analyzing PDV interferograms with a short-time Fourier transform (STFT) with 156 data points (15.6 ns) and a 155 data-point overlap (0.1 ns spacing) Hamming window function[18),19)]. The LiF window was X-cut single crystal with the [100] crystallographic axis aligned along the normal to the PBX-I/LiF window interface. The 10-mm-thick window was mounted along the line BB' as shown in Figure 1. A 0.6-μm-thick aluminum foil was deposited on the window face next to the explosive by radio-frequency magnetron sputtering to provide a reflective surface. The aluminum layer is thin enough (< 1μm) and has a shock impedance close to that of LiF window to introduce negligible perturbations into the flow and interface velocity histories. A single-mode optical fiber was directed to the center point O (i.e. the intersection of AA' and BB') and normal to the window surfaceto relay 1550 nm laser beam to illuminate the target and collect reflected beam carrying velocity information (illustrated as PDV in Figure 1 (b)).

Experiments were carefully constructed to hold necessary tolerances and ensure high repeatability.

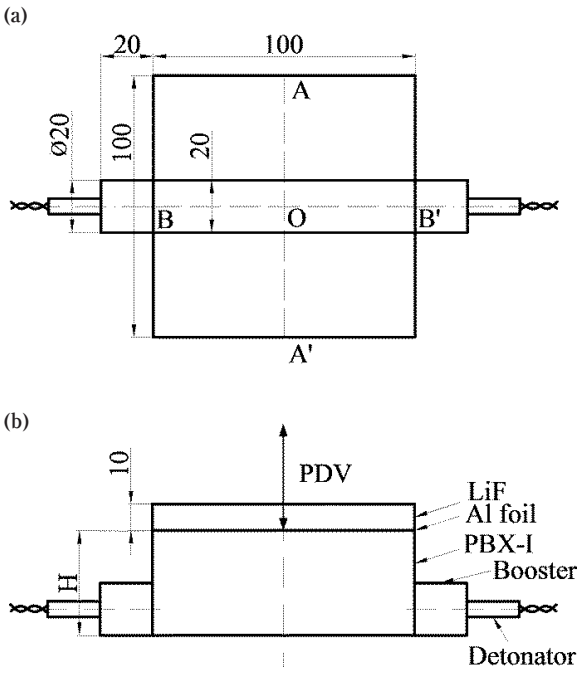

Figure 1 Top view (a) and front view (b) of the experimental setup (unit: mm). H denotes the height of the main charge (20, 40 and 60 mm, respectively).

3. Results and discussion

3.1 Waveform

The detonation wave breakout records from AA' and BB' were shown in Figure 2. The film records were read on a digitized optical comparator, and position data were transformed into times with the still images (not shown in film) and the known camera writing speed. Then the streak records of Figure 2 were digitized and combined to

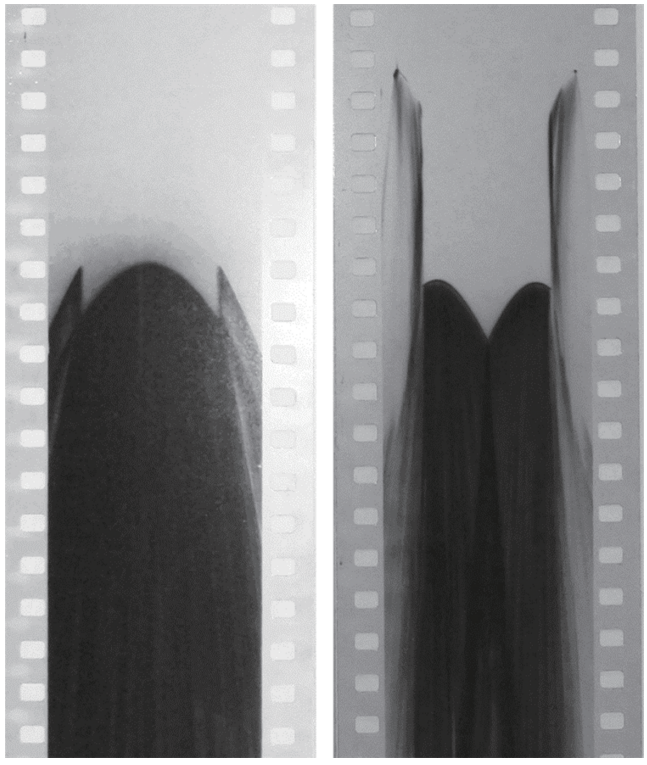

Figure 2 Streak camera records of head-on collision. The left is from AA' – collision line, and the right is from BB' – normal to collision line.

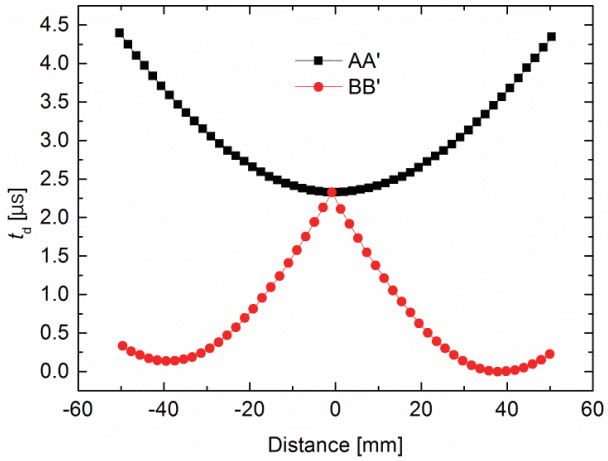

Figure 3 Composite plot for the breakout delay time as a function of the distance.

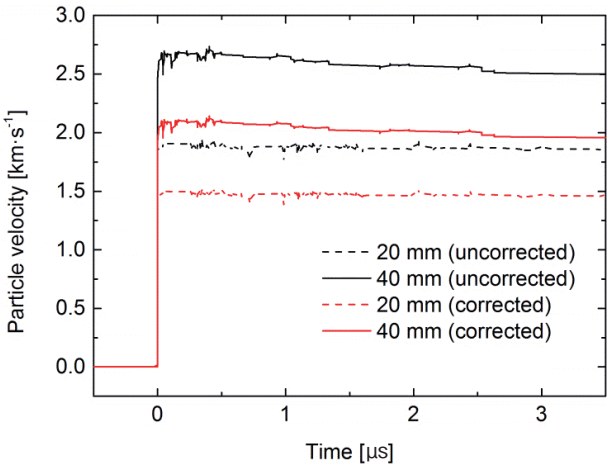

Figure 4 Uncorrected and corrected wave profiles for experiments. The legend denotes the main charge thickness.

produce Figure 3 — a composite plot of delayed time t_d vs. distance. Estimated time resolution was 6 ns. For the reason that AA' and BB' intersect at point O in Figure 1, the two curves representing AA' and BB' in Figure 3 have an intersection, the horizontal coordinate of which is designated as zero. In addition, the time of the first breakout of detonation waves is designated as zero, then the delayed time t_d is defined as the time difference between the time that detonation wave breaking out from the main charge's surface and the first breakout time.

Plot in Figure 3 shows that the two curves are nearly symmetrical with the intersection point. For the curve representing AA', the first breakout of detonation wave comes from the intersection point, i.e. the midpoint of AA', where is nearest to the both initiation positions. Then the detonation wave break outs from the midpoint to the both ends of AA' in chronological order, with the largest time lag of 2.02 μs. Note that the absolute value of the slope increases gradually from the midpoint to the both ends, which means the detonation wave needs more time to break out for the same distance along the collision line. For the curve corresponding to BB', the detonation waves first break out at about 11 mm away from the both ends of BB', where are not the nearest to the initiation positions. This phenomenon is attributed to the corner-turning performance of TATB based explosives[20),21)], which means the dead-zones appear when the detonation waves turn a big corner. Also due to the corner-turning performance, the largest time lag for line BB' is 2.328 μs, which is more than the time lag for line AA'.

3.2 Interface particle velocity

Apparent interface velocity histories are obtained and corrected for the index of refraction of LiF to generate true interface velocity histories[22)]. Both the apparent and true interface velocity profiles are given in Figure 4 with the time zero shifted to the instant when the shock wave reaches the interface between main charge and LiF. Now we just focused on the true velocity profiles. The velocity profiles show an upward trend with increased run of detonation waves (i.e. thickness of the main charge). Note that both the velocity profiles are smooth without any stages, which indicates that the gauging point is exactly on the collision line and subjected two head-on detonation waves simultaneously.

Table 1 Detonation pressure calculations.

Main charge thickness [mm]	First peak true particle velocity [km·s^{-1}]	Peak incident pressure [GPa]
20	1.463	24.28
40	2.099	37.16

LiF is an inert material with a higher shock impedance than the main charge, thus a strong shock is reflected back into the reacting explosive. We can do impedance analysis on the measured point at the explosive-window interface. Using the linear Hugoniot relationship of LiF, which is established from the experimental relation of shock velocity U_s and particle velocity u as[23)]

$$U_s = 5.201 + 1.323u \tag{1}$$

The impedance match equation was then used to calculate the incident or detonation pressure[24)]. The impedance equation is

$$P_i = u\,(\rho_0 U_s + \rho_{HE} D)/2 \tag{2}$$

where P_i is the incident or detonation pressure, ρ_0 the initial density of LiF (2.64 g·cm^{-3}), D is the detonation velocity of the explosive (7.57 km·s^{-1}), ρ_{HE} is the initial density of the explosive.

The first peak true particle velocity in Figure 4 was chosen to calculate the peak incident pressure. The detonation pressure calculation results are shown in Table 1. The incident detonation pressure is less than twice the Chapman–Jouguet (CJ) detonation pressure of PBX-I (29.5 GPa), thus we have reason to believe that the colliding detonation waves are unsteady and not fully built up. And that is why thicker charge need to be investigated in the future.

4. Conclusion

We have performed head-on collisions of detonation

waves experiments for a TATB based IHE in order to get the waveform, interface velocity histories and pressure in the collision region. The experimental setup was well-designed to get accurate results.

The waveform breaking out from the collision line and the line normal to the collision line was recorded respectively by a high-speed streak camera. The breakout delay time as a function of the distance was calculated and shows that and the corner-turning phenomenon was observed from the breakout delay time plots. The interface velocity histories of the center point for two different detonation wave run distances were acquired by PDV system. Results show that this point is just on the collision line and no second stage was observed along the histories. Finally, the incident detonation pressure of the center point was calculated according to the impedance match equation and is less than twice CJ detonation pressure, which indicates the colliding detonation waves are not fully built up. We expect these results to be useful in explosive-driven system. Next step we will conduct further experiments with thicker explosive charges and more velocity measuring points.

Ackonwledgments

This research is funded by the National Natural Science Foundation of China (Nos. 11702265, 11602238).

References

1) C. S. Montross, V. Florea, and J. A. Bolger, Int. J. Rock Mech. Min. Sci., 36, 849−855 (1999).
2) R. Courant and K. O. Friedrichs, "Supersonic flow and shock waves", Interscience (1948).
3) A. H. Shapiro, "The dynamics and thermodynamics of compressible fluid flow", John Wiley & Sons (1953).
4) I. I. Glass and G. N. Patterson, J. Aeronaut. Sci., 22, 73−100 (1955).
5) I. I. Glass and L. E. Heuckroth, Phys. Fluids, 2, 542−546 (1959).
6) T. Minota, M. Nishida, and M. G. Lee, Fluid Dyn. Res., 22, 43−60 (1998).
7) H. D. Ng, B. B. Botros, J. Chao, J. M. Yang, N. Nikiforakis, and J. H. S. Lee, Shock Waves, 15, 341−352 (2006).
8) A. K. Oppenheim, J. J. Smolen, D. Kwak, and P. A. Urtiew, Proc. 5th Symposium (International) on Detonation, 119−136, Office of Naval Research, Arlington (1970).
9) W. S. Vogan, W. W. Anderson, M. Grover, J. E. Hammerberg, N. S. P. King, S. K. Lamoreaux, G. Macrum, K. B. Morley, P. A. Rigg, G. D. Stevens, W. D. Turley, L. R. Veeser, and W. T. Buttler, J. Appl. Phys., 98, 113508 (2005).
10) M. B. Zellner, M. Grover, J. E. Hammerberg, R. S. Hixson, A. J. Iverson, G. S. Macrum, K. B. Morley, A. W. Obst, R. T. Olson, J. R. Payton, P. A. Rigg, N. Routley, G. D. Stevens, W. D. Turley, L. Veeser, and W. T. Buttler, J. Appl. Phys., 102, 013522 (2007).
11) T. Hiroe, K. Fujiwara, H. Hata, and K. Sashima, Sci. Tech. Energetic Materials, 69, 76−81 (2008).
12) V. A. Ogorodnikov, A. L. Mikhaĭlov, V. V. Burtsev, S. A. Lobastov, S. V. Erunov, A. V. Romanov, A. V. Rudnev, E. V. Kulakov, Y. B. Bazarov, V. V. Glushikhin, I. A. Kalashnik, V. A. Tsyganov, and B. I. Tkachenko, J. Exp. Theor. Phys., 109, 530−535 (2009).
13) G. Dimonte, G. Terrones, F. J. Cherne, T. C. Germann, V. Dupont, K. Kadau, W. T. Buttler, D. M. Oro, C. Morris, and D. L. Preston, Phys. Rev. Lett., 107, 264502 (2011).
14) S. K. Monfared, D. M. Oró, M. Grover, J. E. Hammerberg, B. M. LaLone, C. L. Pack, M. M. Schauer, G. D. Stevens, J. B. Stone, W. D. Turley, and W. T. Buttler, J. Appl. Phys., 116, 063504 (2014).
15) Y. Chen, G. Ren, T. Tang, Q. Li, and H. Hu, Shock Waves, 26, 221−225 (2016).
16) M. Singh, H. R. Suneja, M. S. Bola, and S. Prakash, Int. J. Impact Eng., 27, 939−954 (2002).
17) C. Zhang, H. Hu, T. Tang, X. Sun, and Z. Zhang, AIP Conf. Proc., 1426, 1129−1132 (2012).
18) B. J. Jensen, D. B. Holtkamp, P. A. Rigg, and D. H. Dolan, J. Appl. Phys., 101, 013523 (2007).
19) D. H. Dolan, Rev. Sci. Instrum., 81, 053905 (2010).
20) P. C. Souers, S. R. Anderson, B. Hayes, J. Lyle, E. L. Lee, S. M. McGuire, and C. M. Tarver, Propellants Explos. Pyrotech., 23, 200−207 (1998).
21) X. L. Guo, W. Cao, Y. L. Duan, Y. Han, J. L. Ran, and X. J. Lu, Combust. Explos. Shock Waves, 52, 719−726 (2016).
22) P. A. Rigg, M. D. Knudson, R. J. Scharff, and R. S. Hixson, J. Appl. Phys., 116, 033515 (2014).
23) Q. Liu, X. Zhou, X. Zeng, and S. N. Luo, J. Appl. Phys., 117, 045901 (2015).
24) J. K. Rigdon and I. B. Akst, Proc. 5th Symposium (International) on Detonation, 59−66, Office of Naval Research, Arlington (1970).